An XMM-Newton study of several non-radiative filaments in the northeastern rim of the Cygnus Loop

Horvat J., Onić D., Anđelić M., Urošević D.

jasmina.horvat@matf.bg.ac.rs

Department of Astronomy, Faculty of Mathematics, University of Belgrade, Serbia

INTRODUCTION

The Cygnus Loop is a Galactic supernova remnant (SNR). Recently, its distance was estimated to be 725 ± 15 pc [2], based on the parallaxes of the stars available in the Gaia Early Data Release. The most recent estimations shows that this SNR is ~20 000 years old. Cygnus Loop has a very complex morphology, where we can see both radiative and non-radiative optical filaments. Recently, the shock velocity of several optical filaments was calculated from the measured proper motion [8]. Although it isn’t completely excluded, it’s worth noting that it has been suggested recently that the long suspected progenitor generated cavity walls appear, in fact, to be simply discrete interstellar clouds in the remnant’s vicinity [2].

The X-ray boundary in the northeastern rim of the Cygnus Loop is associated with Balmer-dominated filaments which mark current locations of the blast wave [3,5]. X-ray spectroscopic measurements of the Cygnus Loop SNR also indicate that the metal abundances throughout most of the remnant’s rim are depleted to ~0.2 times the solar value (the so called normal abundances) [4]. Recent X-ray studies have revealed in several small regions along the outermost rim the so called enhanced abundances (up to ~1 solar)[4]. These enhanced abundance regions coincide with B and C group of filaments analyzed in [8].

Charge exchange (CX) is a special case of inelastic collision in which one or more electrons is exchanged between an ion and typically a neutral atom, most likely hydrogen [6]. CX is an important process in shock physics because it indicates an interaction between downstream ions and ambient neutral hydrogen, suggesting the presence of a collisionless shock [7]. If the capturing ion is highly ionized then the cascading is expected to result in X-ray line emission. The thin post-shock region of SNRs is a very promising site for possible CX emission. In fact, the presence of CX emission could lead to the inference of apparently enhanced metal abundances using just a pure thermal emission SNR models. Accounting for CX emission in these regions, the actual metal abundances could actually be uniformly low throughout the whole rim.

OBSERVATION AND DATA REDUCTION

The archival XMM-Newton dataset covering the northeastern limb of the Cygnus Loop SNR, Observation ID 0741820101 (P7 region), was downloaded from the XMM-Newton Science Archive and analyzed using standard tools in the HEASOFT Software Package and the Science Analysis Software (SAS) software package. Observation was performed in full frame mode using the thin filter. The processing of the data was done using the latest calibration files available. Particularly, the Extended Source Analysis Software package (ESAS) tools were used to apply standard processing of the PN, MOS1, and MOS2 datasets and to filter the datasets for background flaring activity. After processing, the effective exposure times of the PN, MOS1, and MOS2 cameras were 70.77 ks, 90.75 ks, and 93.50 ks, respectively. In Figure 1 we present an exposure-corrected and adaptively-smoothed combined EPIC (PN+MOS1+MOS2) image of the northeastern limb of the Cygnus Loop, that cover B and C optical filaments from [8], over the energy range from 0.4 keV to 5.0 keV (blue). Hα emission associated with non-radiative filaments is in green. In Figure 2 we can see the three-color image of the same area, with different regions used for spectral analysis, marked with different rectangles. Energy bands are represented by different colors; red: 0.4 – 0.52 keV; green: 0.52 – 1.07 keV; blue: 1.07 – 5.00 keV.

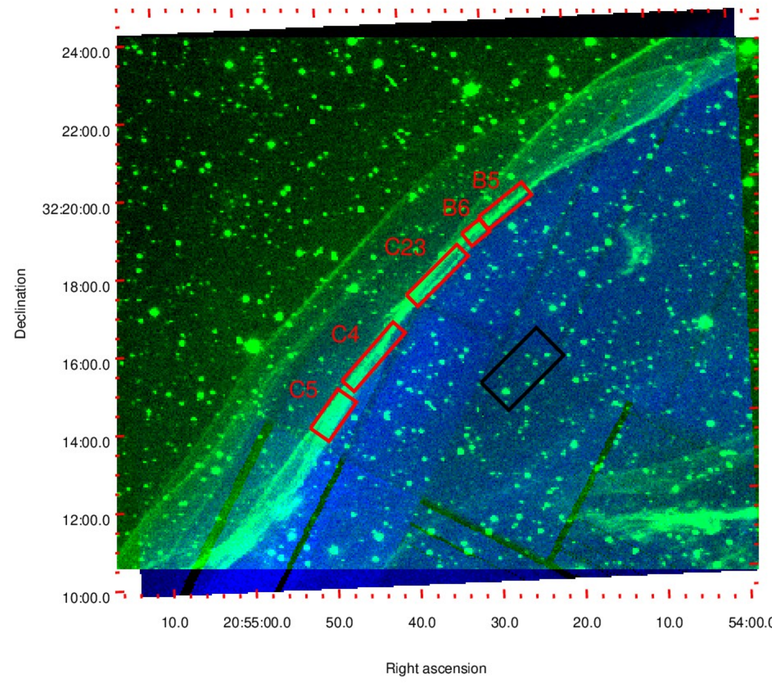

Figure 1: An exposure-corrected and adaptively-smoothed combined EPIC image of the northeastern limb of the Cygnus Loop (blue). Hα emission associated with non-radiative filaments is in green. Red rectangles represent the regions of SNR that we use for spectrum analysis.

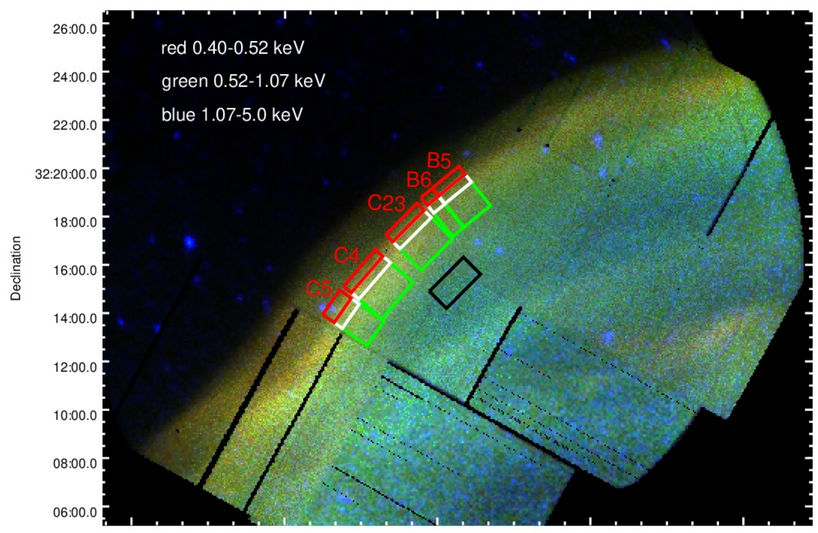

Figure 2: Three-color combined EPIC image of the P7 area of Cygnus Loop, with different regions used for spectral analysis, marked with different rectangles. Energy bands are represented by different colors; red: 0.4 – 0.52 keV; green: 0.52 – 1.07 keV; blue: 1.07 – 5.00 keV.

RESULTS

Here, we present the spatially resolved X-ray spectral analyses of several regions in the northeastern rim of the Cygnus Loop SNR, using the data from MOS 2 camera. The red rectangles in Figure 2 are the regions associated with the filaments itself (c regions), defined in [8]. On the other hand, the white ones correspond to the parts of the SNR in the 25" range behind the optical filaments (b regions). The green regions start after 25" and extend up to 75" (z regions). Finally, the black region represents the area that is not associated with the Hα filament and serves to compare the spectra.

The rim regions can be well fitted by a one-component temperature model with relatively low electron temperature (~0.2 keV). The origin of the plasma in this area is not ejecta. We fit the regions with an absorbed VPSHOCK model with a fixed hydrogen column density for the intervening material of the Cygnus Loop of 3×10^{20} cm^{-2}. This value is much smaller than the total Galactic column density of 1.7×10^{21} cm^{-2} for the direction of the Cygnus Loop. In this simple analysis, we consider that the Solar wind CX is negligible because of the prominent surface brightness of the SNR. The spectra were fitted using the newest version of XSPEC. As this model was not able to fully describe the results, we also included CX emission represented by simple Gaussian lines as in [1].

In Figures 3-5, the X-ray spectra of particular B and C regions are shown with the appropriate best model. It turns out that by including CX emission in the model, abundances are similar to the rest of the rim, except Si and S for which we get systematically higher abundances. So, the CX likely contributes to the X-ray spectrum of the Cygnus Loop from 0.3 to 2.0 keV. We confirm that the abundance-enhanced region is concentrated at least in a ~200" thickness region behind the shock front as noted in [3]. The ionization age increases with distance from the filaments (from the c to the z regions). The plasma is not in CIE, except for B6z and C4z. The electron temperature is around 0.2 keV, but we can not detect any trend with increasing distance from the filaments, probably due to the simplified model and data analysis.

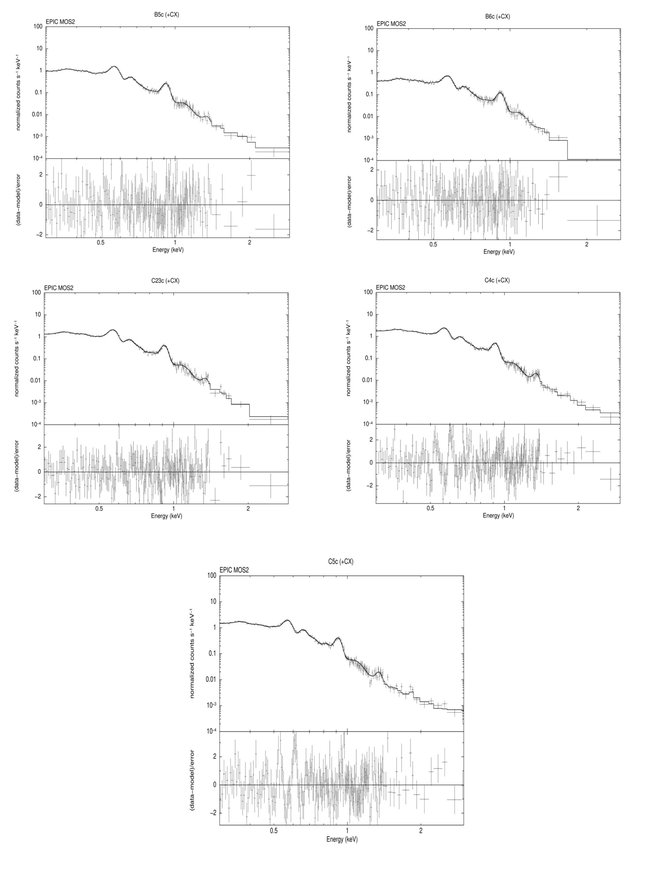

Figure 3: X-ray spectra of the B5c, B6c, C23c, C4c, and C5c regions that coincide with optical filaments. The black line represents the best fit model including CX emission.

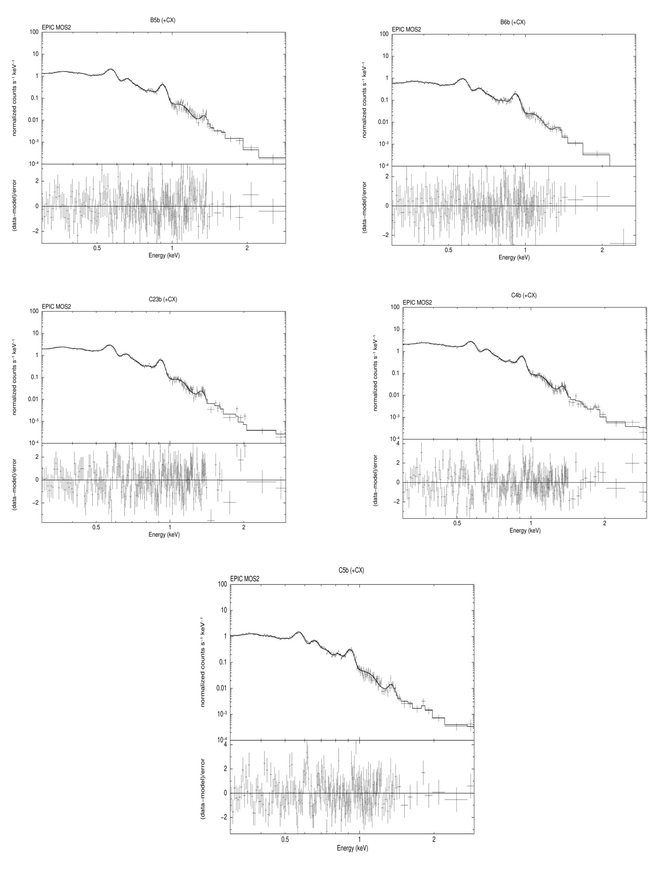

Figure 4: Spectra of the B5b, B6b, C23b, C4b, and C5b regions that coincide with optical filaments. The black line represents the best fit model including CX emission.

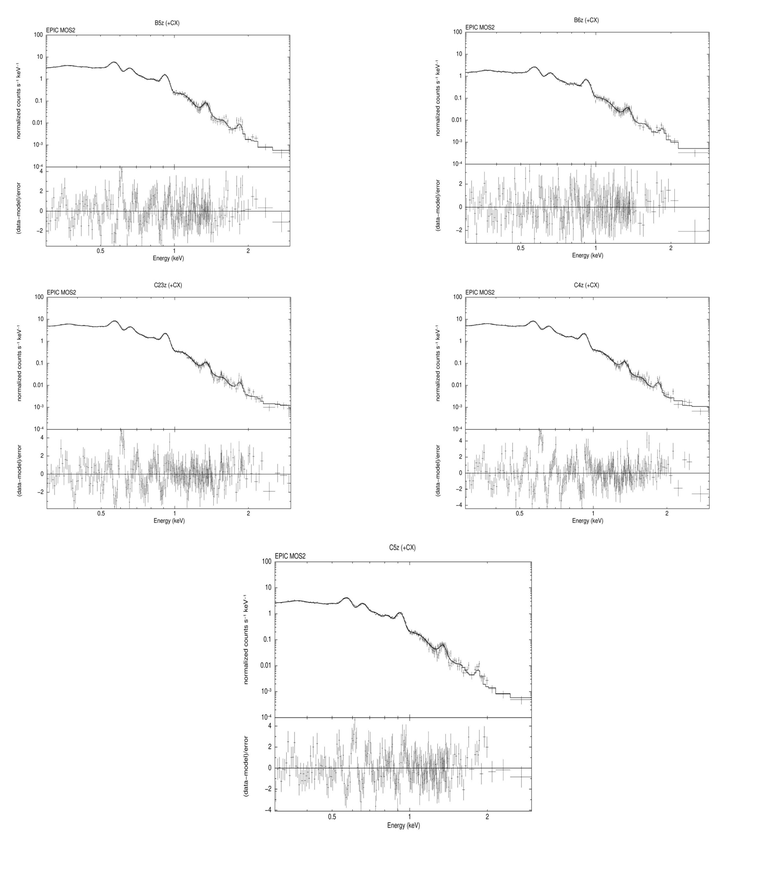

Figure 5: Spectra of the B5z, B6z, C23z, C4z, and C5z regions that coincide with optical filaments. The black line represents the best fit model including CX emission.

DISCUSSION

The results in this paper are generally consistent with the spectral analysis achieved using the data from Suzaku observatory [1,4,6]. However, since the observations made with XMM-Newton are of much lower spectral resolution than those achieved with Suzaku, many emission lines are not resolved. Nevertheless, it turns out that by introducing CX lines into the model, the abundances of most elements decrease and tend towards the so called normal abundances. Discrepancies are most likely due to the simplistic model of CX emission. Recombination rates of ions increase due to CX processes and thus plasmas showing CX emission may be in lower ionization states than those showing pure thermal emission [4]. In that sense we plan to use the more appropriate model that include CX contribution to the X-ray emission of SNRs, in future work.

References

[1] Cumbee, R. S., Henley, D.~B., Stancil, P. C., Shelton, R. L., Nolte, J. L., Wu, Y., Schultz, D. R., 2014, *Astrophys. J.*, 787, L31
[2] Fesen, R. A., Weil, K. E., Cisneros, I., Blair, W. P., Raymond, J. C., 2021, *Mon. Not. R. Astron. Soc.*, 507, 244
[3] Katsuda, S., Tsunemi, H., Kimura, M., Mori, K., 2008, *Astrophys. J.*, 680, 1198
[4] Katsuda, S., Tsunemi, H., Mori K., et al., 2011, *Astrophys. J.*, 730, 24
[5] Nemes, N., Tsunemi, H., Miyata, E., 2008, *Astrophys. J.*, 675, 1293
[6] Roberts, S. R., Wang, Q. D., 2015, *Mon. Not. R. Astron. Soc.*, 449, 1340
[7] Uchida, H., Katsuda, S., Tsunemi, H., Mori, K., Gu, L., Cumbee, R. S., Petre, R., Tanaka, T., 2019, *Astrophys. J.*, 871, 234
[8] Vučetić, M., Milanović, N., Urošević, D., Raymond, J., Onić, D., Milošević, S., Petrov, N., 2023, *Serb. Astron. J.*, 207, 9

Acknowledgement

We acknowledge the funding provided by the Ministry of Science, Technological Development and Innovation of the Republic of Serbia through the contract# 451-03-66/2024-03/200104.